State-to-State Quantum Dynamical Study of the N + OH → NO + H Reaction

M. Jorfi and P. Honvault*

Institut UTINAM, UMR CNRS 6213, University of Franche-Comté, 25030 Besançon Cedex, France

Received: December 19, 2008; Revised Manuscript Received: January 20, 2009

We have studied the quantum dynamics of the N + OH → NO + H reaction for collision energies up to 0.7 eV. The hyperspherical method has been used in a time-independent formalism. State-to-state reaction probabilities for a total angular momentum $J = 0$ have been computed. The results show a high reactivity below 0.45 eV and a very small one above this collision energy. Rotational and vibrational product distributions are presented for three collision energies (0.05, 0.1, and 0.5 eV). The vibrational distributions are found to be noninverted at 0.1 eV and inverted peaking at other energies. Rotational distributions are rather hot even if some low rotational states are strongly populated. These features are consistent with both direct and indirect reaction mechanisms.

1. Introduction

Radical−radical reactions, such as reactive collisions between open-shell atoms (C, N, O) and the hydroxyl radical OH, play a crucial role in the atmospheric chemistry of the Earth[1] and in astrochemistry.[2] Theoretical and experimental studies of these reactions remain a challenging task and are still scarce nowadays. From a theoretical point of view, such systems with two heavy atoms usually involve potential energy surfaces (PES) which present deep potential wells. Many channels thus have to be considered to get converged results. After our studies on O + OH,[3−5] and its reverse H + O_2,[6,7] and C + OH,[8−10] we focus here on the reaction of OH with a nitrogen atom in its ground state, i.e., N (^{4}S) + OH ($^2\Pi$) → NO ($^2\Pi$) + H (^{2}S).

This reaction is involved in the chemistry of NO in the interstellar medium (ISM).[11,12] If we accept the current models of interstellar clouds, the major source of nitric oxide which has been detected by several groups[13−15] is the reaction N + OH → NO + H and another source is O + NH → NO + H. The main destruction reaction is N + NO → N_2 + O. Thus, the N + OH reaction is also a key elementary process of the chemistry of N_2 (recently observed in the ISM).[16] Indeed the formation of N_2 is controlled by the title reaction and the N + NO reaction. These reactions also initiate the formation of ammonia. The N + OH reaction is also important in the combustion of nitrogen-containing fuels[17] and of great importance in the oxidation of atmospheric nitrogen and in the environment as a source of the NO pollutant.

Only a few experiments have been carried out for the title reaction. Smith and co-workers[18−20] have obtained experimental rate constants using a discharge-flow and flash photolysis techniques. They measure the rate constant down to 103 K.[20] They found that the rate increases as the temperature decreases. Experimental vibrational distribution of the NO product has also been measured by laser-induced fluorescence spectroscopy,[21] and it was found somewhat hotter than statistical. Theoretical approaches provide an attractive alternative to study in detail the N + OH reaction and to elucidate its reaction dynamics. Several groups reported electronic structure calculations for the NOH system.[22,23] In particular, Pauzat et al.[22] have characterized the reaction pathway for the N + OH reaction. The first realistic global NOH ground PES for use in dynamics calculations of the title reaction was published in 1995.[24] It was based on CASSCF/internally contracted configuration interaction calculations. Several theoretical rate constants have been calculated using the QCT method,[25] the TDWP quantum method,[26,27] and other approximate methods, such as the statistical adiabatic channel model (SACM)[28] and the adiabatic capture centrifugal sudden approximation (ACCSA) method.[29] Very recently, we have performed a QCT study of the N + OH reaction and gave the rate constant in a wide temperature range.[41]

The N + OH → NO + H reaction which belongs to the class of H + HL → HH + L reactions is highly exothermic by 1.99 eV. The $^3A''$ PES of Guadagnini et al.[24] which corresponds to the ground electronic state of NOH was used in this work. This PES presents no barrier relative to the entrance channel and a double well along the reaction path which correspond to the HON and HNO species. However, it has been shown that the title reaction leads to the initial formation of an HON complex[24] bound by about 3.07 eV relative to the entrance channel. The reactant channel N(^{4}S) + OH(X $^2\Pi$) generates four PESs, namely, $^3A'$, $^3A''$, $^5A'$, and $^5A''$. Only the triplet surfaces can correlate to the ground state of the products, i.e., NO(X$^2\Pi$) + H(^{2}S). The $^3A'$ surface is known to be strongly repulsive in the products channel.[30] Therefore, the $^3A''$ PES is the only surface which is involved at low energies between the ground states of the reagents and products. Details of this PES are given in ref.[24]

Some of the theoretical studies mentioned above also reported quantum-mechanical (QM) total reaction probabilities[26,27] using a TDWP method which is not well adapted to the low energies because of an incomplete damping of the slowly moving components of the wave packet. However there is no quantum study of the product distributions. In particular no QM state-to-state reaction probabilities have been published for the title reaction, although we know that the deepest possible understanding (how energy actually flows among the different degrees of freedom of the products and how chemical reactions actually take place) of reaction dynamics requires full-dimension QM state-to-state calcula-

* Corresponding author, pascal.honvault@univ-fcomte.fr (P. Honvault).

10.1021/jp811237z CCC: $40.75
Published on Web 02/25/2009

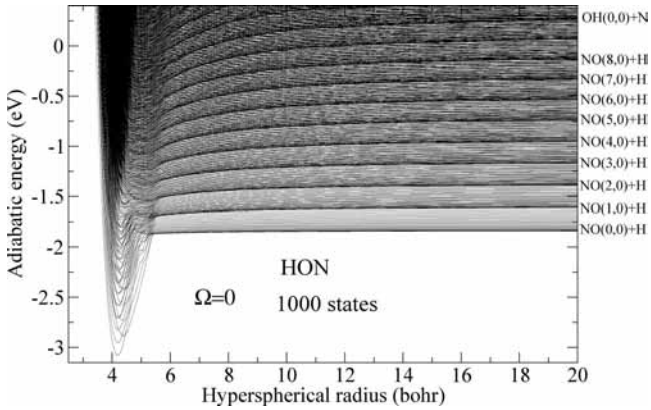

Figure 1. HON hyperspherical adiabatic energies for the $^3A''$ state as a function of hyperspherical radius ρ. The zero point of the energy is taken at the asymptotic minimum of the N + OH channel.

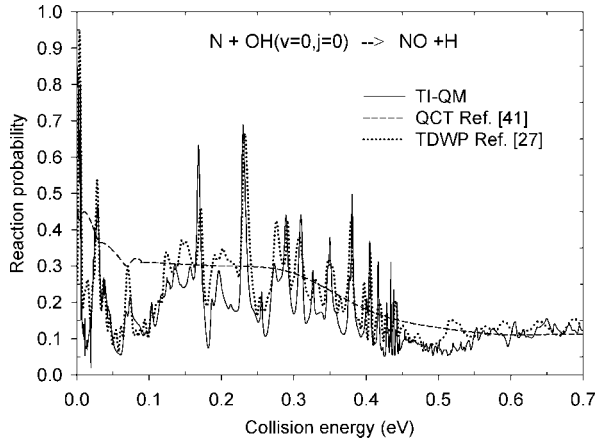

Figure 2. Total reaction probability as a function of the collision energy for the N + OH ($v = 0, j = 0$)→ NO + H reaction.

tions or state-to-state measurements. Furthermore, detailed comparisons between state-to-state QM results and the measurements from high-resolution experiments allow us to improve our knowledge of the chemical reactions. For instance, only a state-to-state QM study can answer fundamental questions, such as the question of whether the vibrational or rotational distributions of the product states are statistically or dynamically controlled. The features of the N + OH reaction yield a great challenge for accurate quantum dynamical calculations. First, the deep potential well and the heavy oxygen and nitrogen masses necessitate a large quantum basis set. Second, many partial waves have to be included for this barrierless reaction, and the floppy nature of the HON complex entails strong Coriolis coupling. In the present work, the title reaction has been studied at the state-to-state level. We have performed time-independent quantum-mechanical (TIQM) calculations of state-to-state reaction probabilities for a total angular momentum $J = 0$ for collision energies up to 0.7 eV. Vibrational and rotational product distributions are also reported.

2. Quantum Mechanical Method

All the QM scattering calculations have been performed on the $^3A''$ PES determined by Schatz and co-workers[24] using a TIQM method. Details of the hyperspherical method can be found in ref 31, and only a brief description is given here. This method has previously proved successful in describing the quantum dynamics of atom−diatom insertion reactions such as $N(^2D) + H_2 \rightarrow NH + H$,[32,33] $O(^1D) + H_2 \rightarrow OH + H$,[34,35] $C(^1D) + H_2 \rightarrow CH + H$,[36] $S(^1D) + H_2 \rightarrow SH + H$,[37] the O + OH reaction,[3−5] the H + O_2 reaction,[6,7] and also ultracold alkali−dialkali collisions.[38,39] Nuclear motion in the NOH system is represented by a set of coordinates which are a modified version of the Smith−Whitten democratic coordinates. They consist of three Euler angles, representing the orientation of the triatomic system in space and three internal coordinates: the hyperradius ρ, which characterizes the size of the system, and two hyperangles (θ, ϕ), which characterize its shape. We first determined a set of surface states $\Phi_k(\rho; \theta, \phi)$, eigenfunctions of a fixed- ρ reference Hamiltonian which incorporates the kinetic energy arising from deformation and rotation at fixed hyperradius around the axis of least inertia, and the potential energy. The Φ_k states were expanded on a basis of pseudo-hyperspherical harmonics. The system N + OH is the most difficult and demanding ever studied among the atom + OH reactions in quantum dynamics calculations, because the three atoms are different and so there is no permutation symmetry, in contrast with the O + OH system.[3−5] Essentially we have to check two crucial parameters for convergence, the number of states (the size of the basis sets), and the asymptotic matching distance. For the $J = 0$ partial wave, the scattering wave function was expanded on a basis with 1000 states Φ_k dissociating at large hyperradius into the NO (110, 106, 101, 96, 91, 85, 79, 72, 65, 57, 48, 37, 21) and OH (14, 3) rovibrational sets (this notation indicates the largest rotational level j for each vibrational manifold v). The range of variation of the hyperradius is divided into 147 equal sectors between 2.9 and 21.1. We then perform a close-coupling expansion of the full NOH wave function onto the surface states. The hyperradial components satisfy a set of second-order coupled differential equations in which all couplings neglected in the first step are taken into account and which arise from the difference between the exact Hamiltonian and the reference Hamiltonian. The logarithmic derivative matrix is propagated inside each sector using the Johnson−Manolopoulos algorithm.[40] Basis transformations are performed at the boundary between sectors and at large hyperradius, the numerically integrated wave function is matched onto a set of regular and irregular asymptotic functions expressed in the laboratory frame. The K and S-matrices are then extracted and state-to-state reaction probabilities are obtained from standard equations.

3. Results and Discussion

The HON hyperspherical adiabatic energies as a function of hyperradius ρ for $\Omega = 0$ (Ω is the projection of the total angular momentum J on the axis of least inertia) are displayed in Figure 1. It shows the large number of channels (1000) which have been considered in this study and exhibits a deep well which is directly linked to the potentiel well of the $^3A''$ PES. The lowest energy has a minimum of about −3.07 eV relative to the N + OH asymptote at $\rho = 4.15a_0$. At large hyperradius, the hyperspherical states describe configurations where an atom is far away from two others, forming a diatomic molecule (OH or NO) lying in a specific rovibrational bound state (v,j). The ($v = 0, j = 0$) state of OH and some rovibrational states of NO are indicated in Figure 1.

State-to-state reaction probabilities which are directly linked to the square modulus of the detailed S matrix elements have been computed for the reaction N + OH (v, j) → NO (v', j') + H at zero total angular momentum ($J = 0$) in the

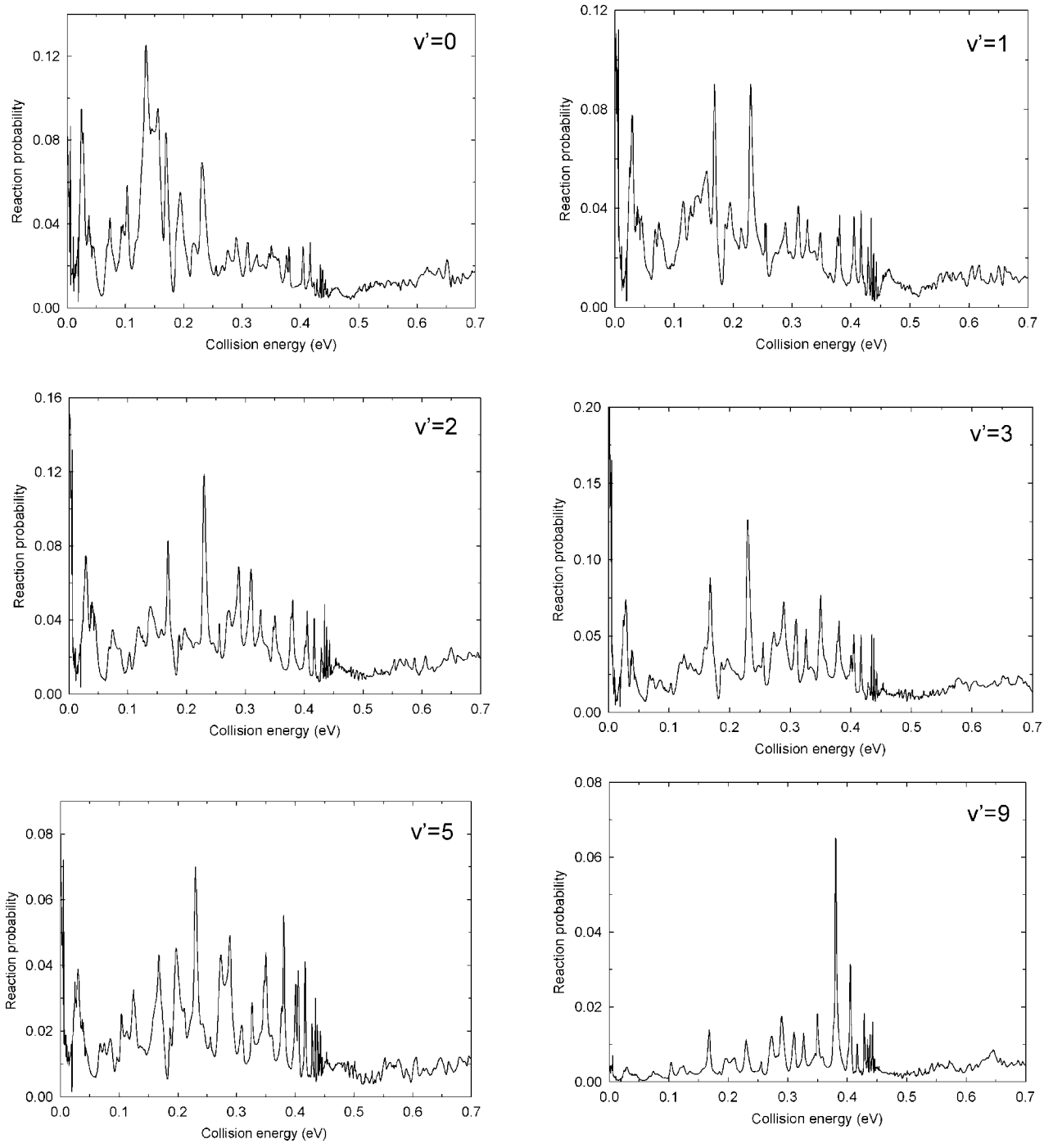

Figure 3. Vibrationally state resolved probabilities as a function of the collision energy for the N + OH ($v = 0, j = 0$)→ NO (v') + H reaction.

0−0.7 eV collision energy range on a regular grid with a step of 0.0005 eV. The total reaction probability is obtained by summing over all open vibrational v' and rotational j' states of NO. In this first accurate quantum study of N + OH, we consider only the reactants in their lowest rovibrational state ($v = 0, j = 0$). Figure 2 shows the total reaction probability as a function of collision energy E_c. The absence of barrier in the PES for the N + OH entrance arrangement leads to a total reaction probability which has no energy threshold. In particular, after the sharp rise at nearly zero energy, we can distinguish two regions, one where the probability is large (for $E_c < 0.45$ eV) and another one where it is twice smaller and almost flat (above 0.45 eV), with an average probability of 0.25 for $0 < E_c < 0.45$ eV and of 0.125 for $0.45 < E_c < 0.7$ eV. These values are relatively low, in contrast to the C + OH case where the probability is close to 1 over the whole energy range considered here. The TIQM curve presents large undulations with some resonances inside. These oscillations average the more numerous structure obtained in the rovibrationaly state-resolved reaction probabilities. However an extremely dense resonant structure is found for collision energies between 0.41 and 0.43 eV. These QM resonances are associated with a long-lived intermediate complex formed in the deep HON well of the PES which supports many quasi-bound states The situtation differs from that found in the O + OH reaction where peaks are very intense and sharp in the whole energy range considered here. This could be explained by the larger exothermicity for the

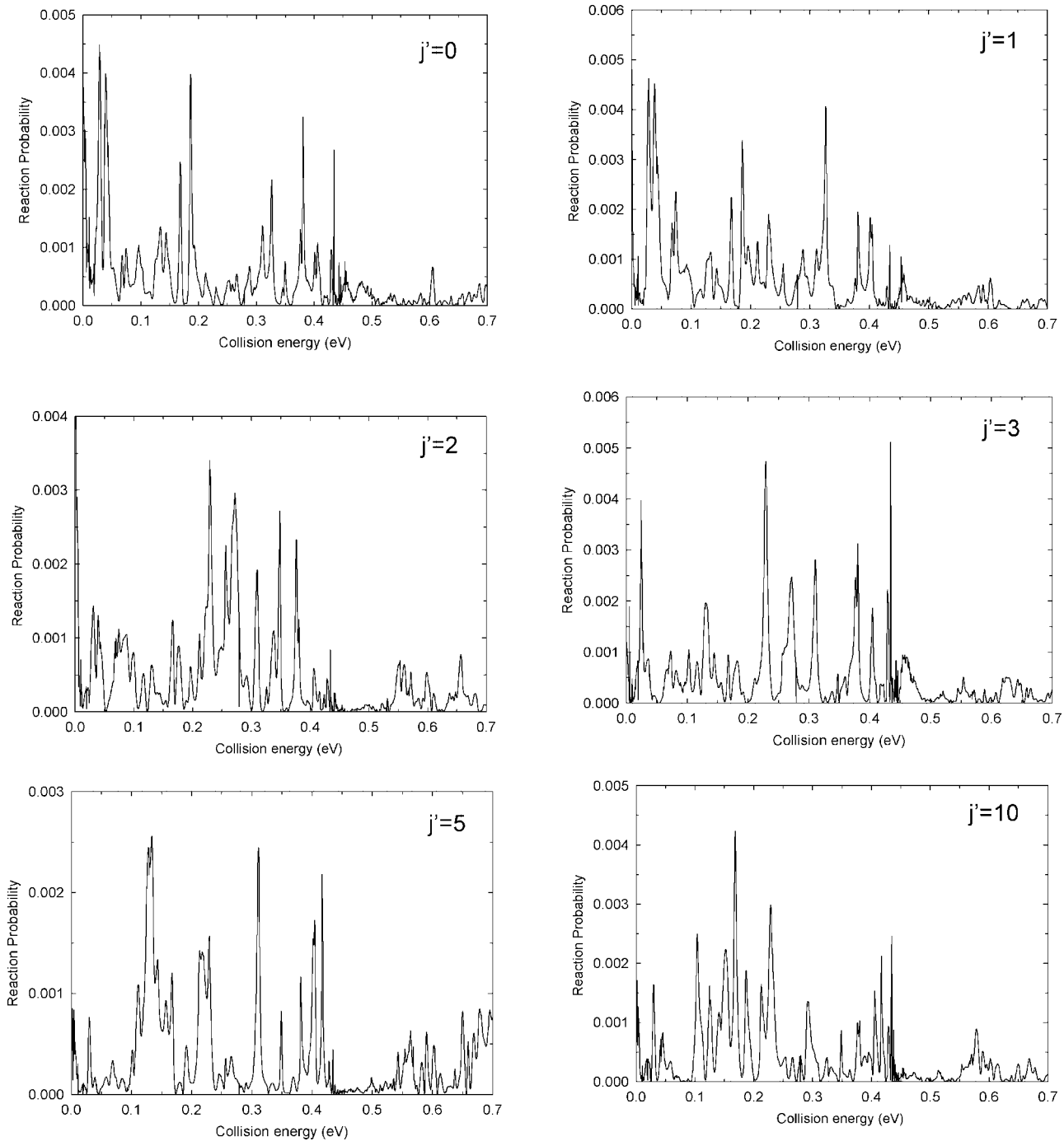

Figure 4. Rotationally state resolved probabilities as a function of the collision energy for the N + OH ($v = 0, j = 0$) → NO ($v' = 1, j'$) + H reaction.

N + OH reaction, 1.99 eV versus 0.71 eV. Indeed a very small exoergicity appears as an essential feature to obtain narrow resonances.[36,37] The reaction probability calculated using a TDWP method[27] is also plotted in Figure 2. TIQM and TDWP approaches yield reaction probabilities which behave very similarly. Apart from slight shifts in some of the resonance peaks and some different magnitudes, both methods provide reaction probabilities in good agreement. However, the TIQM results present a resonance structure which is more pronounced. While no resonances are obtained using the QCT method[41] as expected, a fairly good average description is obtained by the QCT result, and the two regions described above are well visible.

In Figure 3 are shown the vibrationally state resolved reaction probabilities at total angular momentum $J = 0$ calculated in the 0−0.7 eV collision energy range. They are the rotation-summed reaction probability (summed over all open rotational states). Again, for each v', two different regions are clearly visible with the collision energy of 0.45 eV as a separator. The probabilities have similar shapes and a similar resonance structure than for the total reaction probability, with the exception for $v' = 9$ where the probability is high only around 0.4 eV. For this product vibrational state, the reactivity is even the same below 0.4 eV than above 0.6 eV, in contrast with the other v'. The sharp rising of the total reaction probability observed just above $E_c = 0$ eV is present for all vibrationally state resolved probabilities, except again for $v' = 9$. However, for all v', including $v' = 9$, we find again the narrow resonances in the 0.41−0.43 eV energy range.

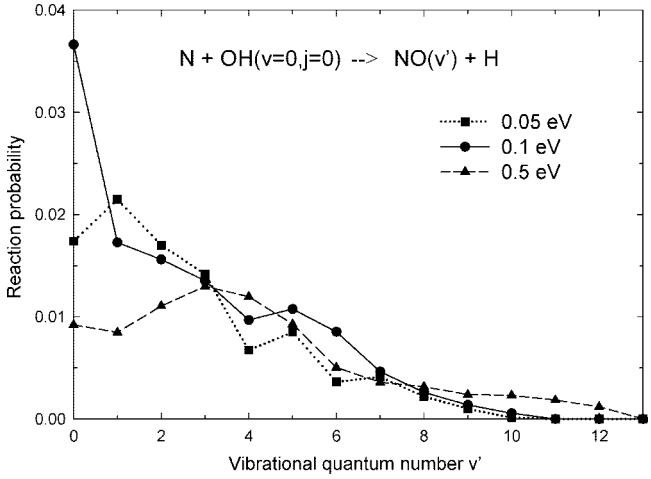

Figure 5. Product vibrational distributions: vibrationally state resolved reaction probabilities as a function of vibrational quantum number v' of NO at 0.05 (dotted line), 0.1 (solid line), and 0.5 eV (dashed line).

Figure 4 shows the rotationally state resolved reaction probabilities for NO ($v' = 1$) as a function of collision energy. As expected, the structures are more narrow than the structures found in the rotation-summed reaction probabilities. It is interesting to notice that at some collision energies, the reaction probability is very small, reaching zero for a few E_c. However, the two regions described above for the total and vibrationally state resolved reaction probabilities are found again. For all j', the resonance structure behaves as for the total and vibrationally state resolved probabilities: numerous pronounced resonances at low energy and broader small resonances at higher energy. There is an exception which is the ($j' = 5$) state where the magnitude is high below 0.55 eV. The magnitudes of rotationally state resolved reaction probabilities are similar. In conclusion, the rotationally state resolved reaction probabilities do not depend strongly on the final rotational state j' of NO. So the reactivity appears to be not rotationally specific. Similar features are obtained for the other v'.

Vibrational distributions (reaction probability as a function of the NO quantum vibrational number v') are plotted in Figure 5 at three collisions energies, 0.05, 0.1, and 0.5 eV. The lowest vibrational states are favored, and the distribution appears to be cold with a probability which is zero above $v' = 12$. However, the behavior is different for each energy. At 0.1 eV, the probability decreases when v' increases, sharply from $v' = 0$ to $v' = 1$ and then smoothly for higher v', with however a small peak at $v' = 5$. This statistical behavior is in good agreement with the QCT result[25] (including all impact parameters b or all J). This feature is similar to the one observed for $O + OH \rightarrow O_2 + H$[42] and for insertion reactions.[32,34] In the last two cases, at all energies considered here, the most populated vibrational level is $v' = 0$, with a decrease which reflects the diminution of open rotational states in a given vibrational manifold and which characterized a statistical behavior. This is not the case at other collision energies, where the vibrational distributions are inverted peaking at $v' = 1$ for 0.05 eV and $v' = 3$ for 0.5 eV. Above $v' = 3$ the distributions have the same shape and magnitude. We see that for $E_c = 0.05$ eV, the vibrational distributions present two other smaller peaks at $v' = 5$ and $v' = 7$. Although there exists an inverted population, our results are not the same as those found for reactions mainly dominated by a direct mechanism, such as $C + OH \rightarrow CO + H$[10] or $F + H_2 \rightarrow HF + H$, which shows a very strong vibrational population inversion. Finally, for the $N + OH \rightarrow NO + H$ reaction, the vibrational distribution is between these two extreme behaviors (statistical or inversion).

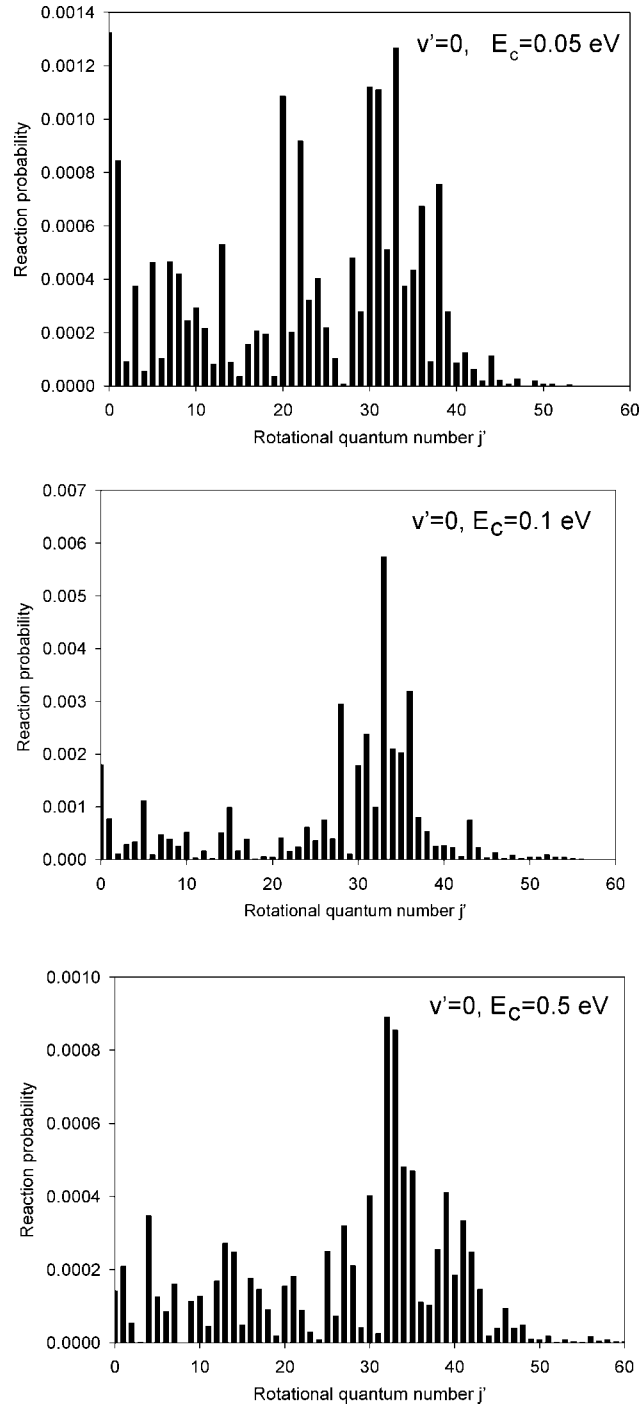

Figure 6. Product rotational distributions: rotationally state resolved reaction probabilities as a function of rotational quantum number j' of NO ($v' = 0$) at 0.05, 0.1, and 0.5 eV.

In Figure 6, we plot the rotational distributions (reaction probability as a function of the NO rotational quantum number j') for NO ($v' = 0$) at three collision energies 0.05, 0.1, and 0.5 eV. The distributions show an oscillatory structure at all collision energies. The main interesting point is the rotational selectivity. All accessible rotational states are not populated, for instance, the probability is nearly zero

at 0.5 eV for $j' = 3$ and 8. At each collision energy, especially at 0.1 eV, only a few rotational states of NO are significantly populated.

Another interesting feature exhibited in Figure 6 is the dependence of product rotational distributions on the collision energy. It is not the same for each collision energy. The most striking effect is seen when the collision energy goes from 0.05 to 0.1 eV. We find that the low states become not populated as the energy increases, yielding a distribution which is very sharp with a maximum for $j' = 33$ at 0.1 eV.

The shape of distributions indicates that the NO product is rather rotationally hot as already found in the O + OH → O_2 + H indirect statistical reaction or in the insertion reactions, such as N (^{2}D) + H_2, although some low states are highly populated at 0.05 eV. They do not behave like those for the C + OH → CO + H reaction,[10] where an increase with j' is found up to a maximum at an intermediate j', with a decrease when the energy of the product states reaches the total energy available. The present distributions have thus neither a statistical nature nor a nonstatistical nature, but a dual nature. In addition, the strong rotational dependence in product state distributions provides additional evidence in support of the mixture between a direct mechanism and complex-forming mechanism.

The rotational distributions for higher vibrational states of NO (not shown here) are essentially unchanged. They sometimes present a slightly different behavior which is always consistent with the contribution of both direct and indirect mechanisms. We find that with increasing product vibrational quantum number (above $v' = 5$), the distributions shift to lower rotational states, even if some high rotational states remain populated.

4. Conclusions

In this paper, we have carried out accurate quantum dynamical calculations of the N + OH → NO + H reaction with the help of an accurate TIQM method. We report exact total and state-to-state QM reaction probabilities for a total angular momentum $J = 0$ using the ab initio PES of Schatz and co-workers.[24] The TIQM total reaction probability calculated for collision energies from 0 to 0.7 eV is in good agreement with those recently obtained with a TDWP method and with the QCT method, although in this last case no sharp peak structure is present. The QM total reaction probability is found to be highly oscillatory due to long-lived resonances supported by the HON potential well. Another important feature is a strong dependence on energy with a large reactivity for collision energies below 0.45 eV and a very small reactivity above this energy. Reaction probabilities for specific rovibrational states have also been computed.The vibrationally state resolved reaction probabilities show the same general picture as the total reaction probabiliy. As expected, a more dense resonance structure is found in rotationally state resolved reaction probabilities. The product vibrational quantum state distributions plotted at three collision energies (0.05, 0.1, 0.5 eV) are rather cold (the lowest vibrational states of NO are favored), even if some of them are inverted peaking. Product rotational distributions at the same energies are highly selective, with a nearly zero reaction probability for some rotational states. Our results show a high rotational excitation in the product state distribution, even if the rotational distribution becomes less hot as the vibrational excitation of NO increases. These state-to-sate calculations obtained for $J = 0$ give results which yield both statistical and nonstatistical product distributions. It thus shows evidence that the title reaction involves both direct and indirect mechanisms.

The present study is limited in the case of $J = 0$ because of the computationally extremely expensive exact QM calculations for the N + OH reaction. Of course there are other significant contributions of nonzero J to the reaction cross section or rate constant, and these higher partial waves have to be taken into account in order to see how large an impact they would have on the reaction dynamics. We would also like to study the initial rotational or vibrational excitation in the OH reactant in order to see their effect on the product distributions. To this end, we plan to perform new accurate QM studies on the same PES for $J = 0$ but with the OH radical in rotational and/or vibrational excited states. We will also try to perform exact quantum calculations for $J > 0$ with OH ($v = 0, j = 0$).

Acknowledgment. M.J. and P.H. acknowledge support from the Institut du Développement des Ressources en Informatique Scientifique (IDRIS) in Orsay (France) and also the UTINAM laboratory for its fast cluster. This work was supported by the Pôle de Sciences Planétaires Bourgogne Franche-Comté.

References and Notes

(1) Wayne, R. P. *Chemistry of Atmospheres*; Oxford University Press, 3rd ed.; New York, 2000.
(2) Carty, D.; Goddard, A.; Kohler, S. P. K.; Sims, I. R.; Smith, I. W. M. *J. Phys. Chem. A* **2006**, *110*, 3101.
(3) Xu, C.; Xie, D.; Honvault, P.; Lin, S. Y.; Guo, H. *J. Chem. Phys.* **2007**, *127*, 024304.
(4) Lin, S. Y.; Guo, H.; Honvault, P.; Xu, C.; Xie, D. *J. Chem. Phys.* **2008**, *128*, 014303.
(5) Jorfi, M.; Honvault, P.; Halvick, P.; Lin, S. Y.; Guo, H. *Chem. Phys. Lett.* **2008**, *462*, 53.
(6) Lin, S. Y.; Guo, H.; Honvault, P.; Xie, D. *J. Phys. Chem. B* **2006**, *110*, 23641.
(7) Honvault, P.; Lin, S. Y.; Xie, D.; Guo, H. *J. Phys. Chem. A* **2007**, *111*, 5349.
(8) Zanchet, A.; Bussery-Honvault, B.; Honvault, P. *J. Phys. Chem. A* **2006**, *110*, 12017.
(9) Zanchet, A.; Halvick, P.; Rayez, J.-C.; Bussery-Honvault, B.; Honvault, P. *J. Chem. Phys.* **2007**, *126*, 184308.
(10) Zanchet, A.; Halvick, P.; Bussery-Honvault, B.; Honvault, P. *J. Chem. Phys.* **2008**, *128*, 204301.
(11) Tarafdar, S. P.; Dalgarno, A. *Astron. Astrophys.* **1990**, *232*, 239.
(12) Gerin, M.; Viala, Y.; Pauzat, F.; Ellinger, Y. *Astron. Astrophys.* **1992**, *266*, 463.
(13) McGonagle, D.; Ziurys, L. M.; Irvine, W. M.; Minh, Y. C. *Astrophys. J.* **1990**, *359*, 121.
(14) Ziurys, L. M.; McGonagle, D.; Minh, Y. C.; Irvine, W. M *Astrophys. J.* **1991**, *373*, 535.
(15) Gerin, M.; Viala, Y.; Casoli, F. *Astron. Astrophys.* **1993**, *268*, 212.
(16) Knauth, D. C.; Andersson, B. G.; McCandliss, S. R.; Warren Moos, H. *Nature* **2004**, *429*, 636.
(17) Miller, J. A.; Bowman, C. T. *Prog. Energy Combust. Sci.* **1989**, *15*, 287.
(18) Howard, M. J.; Smith, I. W. M. *Chem. Phys. Lett.* **1980**, *69*, 40.
(19) Howard, M. J.; Smith, I. W. M. *J. Chem. Soc., Faraday Trans.* **1981**, *77*, 997.
(20) Smith, I. W. M.; Stewart, D. W. A. *J. Chem. Soc., Faraday Trans.* **1994**, *90*, 3221.
(21) Smith, I. W. M.; Tuckett, R. P.; Whitham, C. J. *J. Chem. Phys.* **1993**, *98*, 6267.
(22) Pauzat, F.; Ellinger, Y.; Berthier, G.; G rin, M.; Viala, Y. *Chem. Phys.* **1993**, *174*, 71.
(23) Mordaunt, D. H.; Flothmann, H.; Stumpf, M.; Keller, H. M.; Beck, C.; Schinke, R.; Yamashita, K. *J. Chem. Phys.* **1997**, *107*, 6603.
(24) Guadagnini, R.; Schatz, G. C.; Walch, S. P. *J. Chem. Phys.* **1995**, *102*, 774.
(25) Guadagnini, R.; Schatz, G. C.; Walch, S. P. *J. Chem. Phys.* **1995**, *102*, 784.

(26) Chen, M. D.; Tang, B. Y.; Han, K. L.; Lou, N. Q.; Zhang, J. Z. H. *J. Chem. Phys.* **2003**, *118*, 6852.

(27) Ge, M. H.; Chu, T. S.; Han, K. L. *J. Theor. Comput. Chem.* **2008**, *7*, 607.

(28) Cobos, C. J *Int. J. Chem. Kinet.* **1995**, *27*, 219.

(29) Edvardsson, D.; Williams, C. F.; Clary, D. C. *Chem. Phys. Lett.* **2006**, *431*, 261.

(30) Colton, M. C.; Schatz, G. C. *J. Chem. Phys.* **1985**, *83*, 3413.

(31) Honvault, P.; Launay, J.-M. *Theory of Chemical Reaction Dynamics*; Lagana, A., Lendvay, G., Eds.; Kluwer: Dordrecht, The Netherlands, 2004; p 187.

(32) Honvault, P.; Launay, J. M. *J. Chem. Phys.* **1999**, *111*, 6665.

(33) Balucani, N.; Cartechini, L.; Capozza, G.; Segoloni, E.; Casavecchia, P.; Volpi, G. G.; Aoiz, F. J.; Banares, L.; Honvault, P.; Launay, J.-M. *Phys. Rev. Lett.* **2002**, *89*, 013201.

(34) Honvault, P.; Launay, J.-M. *J. Chem. Phys.* **2001**, *114*, 1057.

(35) Aoiz, F. J.; Banares, L.; Castillo, J. F.; Vallance, C.; Denzer, W.; Brouard, M.; Honvault, P.; Launay, J.-M.; Dobbyn, A. J.; Knowles, P. J *Phys. Rev. Lett.* **2001**, *86*, 1729.

(36) Banares, L.; Aoiz, F. J.; Honvault, P.; Bussery-Honvault, B.; Launay, J.-M. *J. Chem. Phys.* **2003**, *118*, 565.

(37) Banares, L.; Castillo, J. F.; Honvault, P.; Launay, J.-M. *Phys. Chem. Chem. Phys.* **2005**, *7*, 627.

(38) Soldàn, P.; Cvitas, M. T.; Hutson, J. M.; Honvault, P.; Launay, J.-M. *Phys. Rev. Lett.* **2002**, *89*, 153201.

(39) Cvitas, M. T.; Soldàn, P.; Hutson, J. M.; Honvault, P.; Launay, J. M. *Phys. Rev. Lett.* **2005**, *94*, 033201.

(40) Manolopoulos, D. E. *J. Chem. Phys.* **1986**, *85*, 6425.

(41) Jorfi, M.; Honvault, P.; Halvick, P. *Chem. Phys. Lett.* In press.

(42) Jorfi, M.; Honvault, P.; Bargueno de Retes, P.; Gonzalez-Lezana, T.; Larregaray, P.; Bonnet, L.; Halvick, P. *J. Chem. Phys.* In preparation.

JP811237Z